Inorg. Chem. **2005**, *44*, 2606–2618

Low-Coordinate Chromium Siloxides: The "Box" $[Cr(\mu\text{-}Cl)(\mu\text{-}OSi^tBu_3)]_4$, Distorted Trigonal $[(^tBu_3SiO)_3Cr][Na(benzene)]$ and $[(^tBu_3SiO)_3Cr][Na(dibenzo\text{-}18\text{-}c\text{-}6)]$, and Trigonal $(^tBu_3SiO)_3Cr$

Orson L. Sydora,[†] Peter T. Wolczanski,*[,†] Emil B. Lobkovsky,[†] Corneliu Buda,[‡] and Thomas R. Cundari[‡]

Department of Chemistry and Chemical Biology, Baker Laboratory, Cornell University, Ithaca, New York 14853 and Department of Chemistry, University of North Texas, Box 305070, Denton, Texas 76203-5070

Received August 24, 2004

Treatment of $CrCl_2(THF)_2$ with $NaOSi^tBu_3$ afforded the tetrameric "box" $[Cr(\mu\text{-}Cl)(\mu\text{-}OSi^tBu_3)]_4$ (**1**, X-ray). THF cleaved **1** to provide *trans*-(silox)ClCr(THF)$_2$ (**2**), whereas degradation of **1** with 4-picoline caused disproportionation and the generation of *trans*-$Cl_2Cr(4\text{-pic})_2$ and *trans*-$(silox)_2Cr(4\text{-pic})_x$ ($n = 2$, **3**; 3, **3**-4-pic). Chromous centers in **1** were antiferromagnetically coupled, and density functional calculations on the high-spin (multiplicity = 17) model $[Cr(\mu\text{-}Cl)(\mu\text{-}OH)]_4$ (**1′**) revealed that its singly occupied 3d orbitals spanned an energy range of ~2 eV. The addition of 8 equiv of Na(silox) to **1** yielded $[(^tBu_3SiO)Cr(\mu\text{-}OSi^tBu_3)_2]Na\cdot C_6H_6$ (**4**, Y shaped, $\angle OCrO(Na) = 91.28(7)°$), and treatment of **4** with dibenzo-18-crown-6 produced $[(silox)_3Cr][Na(dibenzo\text{-}18\text{-}crown\text{-}6)]$ (**5**, $\angle OCrO = \sim 120°$, $(120 + \alpha)°$, $(120 - \alpha)°$). Calculations of $[(^tBu_3SiO)Cr(\mu\text{-}OSi^tBu_3)_2]Na$ (**4′**) and $Cr(silox)_3^-$ (**5′**) provided reasonable matches with the experimental geometries (X-ray). The trigonal chromic derivative $(silox)_3Cr$ (**6**) was synthesized from $CrCl_3(THF)_3$ for structural and calculational comparisons to the chromous derivatives.

Introduction

In the synthesis of transition-metal complexes, it is crucial to control the steric bulk of a ligand, its bridging capability, and the coordination number to achieve a desired aggregation. As the ligands become sterically larger, lower coordination numbers may be achieved as long as their bridging ability is attenuated. Steric protection of an alkoxide or siloxide via the use of a bulky substituent can often minimize bridging situations.[1] The use of silox (i.e., $^tBu_3SiO$) as an ancillary ligand is predicated on this feature, and a plethora of mononuclear transition-metal complexes have been synthesized, typically with three siloxides within the coordination sphere. As part of these continuing studies, some unusual trigonal species,[2] $(silox)_3M$ (M = Ti,[3,4] V,[4,5] Ta),[1,5,6] have been prepared, but crystallographic confirmation has not been forthcoming, mostly because of twinning complications.

It has been shown that only minor modification (e.g., $^tBu_2RSiO$; R = Me, Ph, etc.) of a tris-siloxide coordination sphere is enough to foment dimerization when the metal is tantalum.[1] Moreover, even with smaller metal centers, if the potential for strong metal−metal bonding exists, then it is difficult to keep bis-silox coordination spheres from dimerizing (e.g., $[(silox)_2H_2Ta]_2$,[7] $(silox)_2ORe{\equiv}ReO(silox)_2$,[8] $(silox)_2XW{\equiv}WX(silox)_2$).[9] This factor has hampered attempts to synthesize certain three-coordinate molecules.

* Corresponding author. E-mail: ptw2@cornell.edu.
† Cornell University.
‡ University of North Texas.

(1) Chadeayne, A. R.; Wolczanski, P. T.; Lobkovsky, E. B. *Inorg. Chem.* **2004**, *43*, 3421−3432.
(2) Cummins, C. C. *Prog. Inorg. Chem.* **1998**, *47*, 685−836.
(3) Covert, K. J.; Wolczanski, P. T.; Hill, S. A.; Krusic, P. J. *Inorg. Chem.* **1992**, *31*, 66−78.
(4) Covert, K. J.; Neithamer, D. R.; Zonnevylle, M. C.; LaPointe, R. E.; Schaller, C. P.; Wolczanski, P. T. *Inorg. Chem.* **1991**, *30*, 2494−2508.
(5) Veige, A. S.; Slaughter, L. M.; Lobkovsky, E. B.; Wolczanski, P. T.; Matsunaga, N.; Decker, S. A.; Cundari, T. R. *Inorg. Chem.* **2003**, *42*, 6204−6224.
(6) Neithamer, D. R.; LaPointe, R. E.; Wheeler, R. A.; Richeson, D. S.; Van Duyne, G. D.; Wolczanski, P. T. *J. Am. Chem. Soc.* **1989**, *111*, 9056−9072.
(7) Miller, R. L.; Toreki, R.; LaPointe, R. E.; Wolczanski, P. T.; Van Duyne, G. D.; Roe, D. C. *J. Am. Chem. Soc.* **1993**, *115*, 5570−5588.
(8) Douthwaite, R. E.; Wolczanski, P. T.; Merschrod, E. *J. Chem. Soc., Chem. Commun.* **1998**, 2591−2592.
(9) (a) Miller, R. L.; Lawler, K. A.; Bennett, J. L.; Wolczanski, P. T. *Inorg. Chem.* **1996**, *35*, 3242−3253. (b) Miller, R. L.; Wolczanski, P. T.; Rheingold, A. L. *J. Am. Chem. Soc.* **1993**, *115*, 10422−10423. (c) Chamberlin, R. L. M.; Rosenfeld, D. C.; Wolczanski, P. T.; Lobkovsky, E. B. *Organometallics* **2002**, *21*, 2724−2735.

10.1021/ic0488334 CCC: $30.25
Published on Web 03/24/2005

Scheme 1

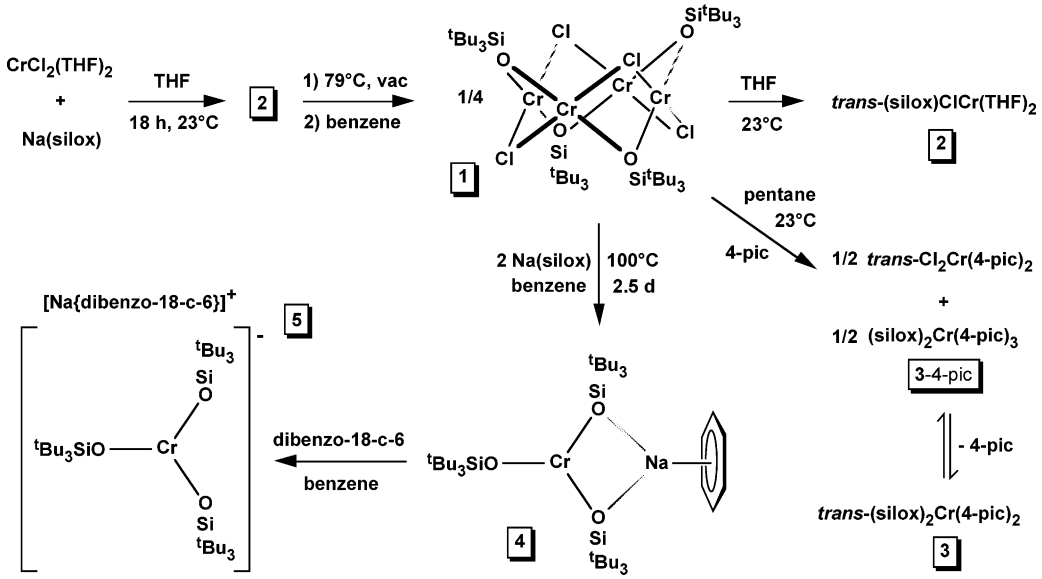

An exploration into the aggregation of $[(^tBu_3SiS)MX]_n$ led to the discovery of a ferrous cube (X = C≡CSi^{t}Bu$_3$, n = 4), ferrous wheels (X = Cl, Br, n = 12), a related ellipse (X = I, n = 14),[10] and cobaltous (X = Cl, n = 12) and nickelous (X = Br, n = 12) wheels.[11] With the thiolate chemistry in mind, the generation and control of "(silox)MX" aggregation was deemed an intriguing synthetic goal. Application of silox to chromium resulted in the formation of an unusual tetramer; a "box" with square-planar "*trans*-(μ-OSi^{t}Bu$_3$)$_2$Cr(μ-Cl)$_2$" sides. The structure and cleavage of the box has been studied, and the complex serves as a starting material for the rare trigonal chromous anion, $[(silox)_3Cr]^-$. Structural characterization of this anion, the first of the "(silox)$_3$M" genre, is reported herein along with pertinent calculations on the chromous compounds.

Results

Chromous Box [Cr(μ-Cl)(μ-OSi^{t}Bu$_3$)]$_4$ (1). 1. Synthesis. Scheme 1 illustrates the preparative chemistry in this chromous system. Treatment of $CrCl_2(THF)_2$ with NaOSi^{t}Bu$_3$ (~0.73 equiv) in THF for 18 h at 23 °C afforded a turquoise solid upon filtration and solvent removal. Use of the siloxide as the limiting reagent helped minimize further metathesis. It seems likely that the turquoise material is *trans*-(^{t}Bu$_3$SiO)CrCl(THF)$_2$ (vide infra). Thermolysis of the material at 79 °C under vacuum for 45 min produced a purple solid that was extracted into benzene and crystallized via slow evaporation to yield purple rods of [Cr(μ-Cl)(μ-OSi^{t}Bu$_3$)]$_4$ (**1**, 78%). The ^{1}H NMR spectrum of **1** revealed a broad resonance ($\nu_{1/2} \approx$ 270 hz) at δ 1.42, and the UV−vis spectrum manifested two bands of modest intensity at 529 (ϵ = 270 M^{-1}cm^{-1}) and 612 nm (260 M^{-1}cm^{-1}), whose intensities were consistent with ligand-field transitions. By assigning the latter band to $\Delta E\{(d_{z^2}{}^1d_{xz}{}^1d_{yz}{}^1d_{x^2-y^2}{}^1) \rightarrow (d_{z^2}{}^1d_{xz}{}^1d_{yz}{}^1d_{xy}{}^1)\} \approx 10$ Dq, the field strength is estimated to be roughly 16 000 cm^{-1}, which is reasonable for Cr(II) in a neutral alkoxide and chloride environment.[12] Initial magnetic studies by Evans' method indicated that substantial Cr···Cr interactions were present because the μ_{eff} was 1.7μ_B at 295 K.[13]

2. Molecular Structure. Details of the data collection and refinement pertaining to [Cr(μ-Cl)(μ-OSi^{t}Bu$_3$)]$_4$ (**1**) are summarized in Table 1, and selected interatomic distances and angles are given in Table 2. Data were collected on several crystals, and an apparent disorder of the silox ^{t}Bu groups, as discerned by high thermal parameters associated with the carbon atoms, was always present. Attempts to model the disorder failed, but although the periphery of the compound is rather poorly defined, the core of the tetrachromous box is devoid of problems (Figure 1). Each chromium atom resides in a pseudo-square-planar environment of two trans chlorides and two trans siloxides that are distorted slightly toward a sawhorse and comprise the sides of the box. The chromiums are positioned slightly toward the outside of the box, with $\angle(Cl-Cr-Cl)_{av}$ = 158.7(5)° and $\angle(O-Cr-O)_{av}$ = 169.7(9)°. The box is slightly flattened, with the side $\angle$O−Cr−Cl pinched down (82.2(3)° av) and the top $\angle$O−Cr−Cl opened up (95.9(9)° av). The d(Cr−O)$_{av}$ of 2.017(21) Å is about 0.10 Å longer than a typical terminal Cr(II) siloxide distance (vide infra) but consistent with its bridging mode (i.e., $\angle(Cr-O-Si)_{av}$ = 137.4(23)°) and minimal π interactions. The bridging d(Cr−Cl)$_{av}$ (2.382(8) Å) is also correspondingly longer, and the generally longer chromium chloride bonds greatly impact the Cr−Cl−Cr (68.5(2)° av) and Cr−O−Cr (83.2(6)° av) angles.

The d(Cr···Cr)$_{av}$ values of 2.679(12) and 3.789(12) Å that correspond to the adjacent and opposite interatomic dis-

(10) Sydora, O. L.; Wolczanski, P. T.; Lobkovsky, E. B. *Angew. Chem., Int. Ed.* **2003**, *4*, 22685−22687.
(11) Sydora, O. L.; Wolczanski, P. T.; Lobkovsky, E. B.; Rumberger, E.; Hendrickson, D. N. *Chem. Commun.* **2004**, 650−651.
(12) Figgis, B. N. *Introduction to Ligand Fields*; Interscience: New York, 1966.
(13) (a) Evans, D. F. *J. Chem. Soc.* **1959**, 2003−2005. (b) Orrell, K. G.; Sik, V. *Anal. Chem.* **1980**, *52*, 567−569. (c) Schubert, E. M. *J. Chem. Educ.* **1992**, *69*, 62.

Table 1. Crystallographic Data for $[Cr(\mu\text{-}Cl)(\mu\text{-}OSi^tBu_3)]_4$ (**1**), $[(^tBu_3SiO)Cr(\mu\text{-}OSi^tBu_3)_2]Na\cdot C_6H_6$ (**4**), $[(^tBu_3SiO)_3Cr][Na(dibenzo\text{-}18\text{-}crown\text{-}6)]$ (**5**), and $(^tBu_3SiO)_3Cr$ (**6**)

	1	**4**	**5**	**6**
formula	$C_{24}H_{54}O_2Si_2Cl_2Cr_2$[a]	$C_{42}H_{87}O_3Si_3NaCr$	$C_{133}H_{231}O_{18}Si_6Na_2\ Cr_2$[b]	$C_{36}H_{81}O_3Si_3Cr$
formula wt	605.75	799.38	2436.8	698.28
space group	*C*2/*c*	$P2_1/n$	$P2_1/n$	*C*2/*c*
Z	8	4	4	8
a, Å	22.333(18)	13.1090(8)	29.194(7)	12.8518(6)
b, Å	13.574(16)	17.0223(13)	17.917(4)	22.6741(12)
c, Å	22.32(2)	22.1690(15)	30.123(7)	29.5161(15)
α, deg	90	90	90	90
β, deg	107.21(4)	94.570(4)	114.744(3)	95.4650(10)
γ, deg	90	90	90	90
V, Å^3	6463(11)	4931.2(6)	14310(6)	8562.0(7)
r_{calcd}, g·cm^{-3}	1.245	1.077	1.131	1.083
μ, mm^{-1}	0.930	0.346	0.266	0.380
temp, K	173(2)	173(2)	173(2)	173(2)
λ (Å)	0.71073	0.71073	0.71073	0.71073
R ind [$I > 2\sigma(I)$][c,d]	$R_1 = 0.1227$	$R_1 = 0.0558$	$R_1 = 0.0722$	$R_1 = 0.0515$
	wR2 = 0.3516	wR2 = 0.1436	wR2 = 0.1950	wR2 = 0.1058
R ind (all data)[c,d]	$R_1 = 0.1698$	$R_1 = 0.0779$	$R_1 = 0.1099$	$R_1 = 0.0808$
	wR2 = 0.3903	wR2 = 0.1578	wR2 = 0.2279	wR2 = 0.1171
GOF[e]	1.450	1.017	0.933	1.073

[a] The asymmetric unit (formula) is one-half of the molecule. [b] The asymmetric unit (formula) contains two molecules and seven benzenes of solvation. [c] $R_1 = \sum||F_o| - |F_c||/S|F_o|$. [d] $wR2 = [\sum w(|F_o| - |F_c|)^2/\sum wF_o^2]^{1/2}$. [e] GOF (all data) $= [\sum w(|F_o| - |F_c|)^2/(n-p)]^{1/2}$, n = number of independent reflections, p = number of parameters.

Table 2. Selected Interatomic Distances (Å) and Angles (deg) for $[Cr(\mu\text{-}Cl)(\mu\text{-}OSi^tBu_3)]_4$ (**1**)

Cr1−Cr3	2.688(3)	Cr2−Cr3	2.670(3)	Cr1−Cr2	2.679(3)
Cr3−Cr3′	3.789(3)	Cr1−O2	2.027(8)	Cr2−O1	1.987(8)
Cr3−O1	2.016(8)	Cr3−O2	2.036(8)	Cr1−Cl2	2.394(4)
Cr2−Cl1	2.378(3)	Cr3−Cl1	2.376(4)	Cr3−Cl2	2.378(4)
Si1−O1	1.694(9)	Si2−O2	1.655(8)	Si−C(ave)	1.93(5)
C−C(av)	1.54(4)				
Cr1−O2−Cr3	82.8(3)	Cr1−Cl2−Cr3	68.34(11)	Cr2−O1−Cr3	83.6(3)
Cr2−Cl1−Cr3	68.56(11)	O2−Cr1−O2′	169.2(4)	O1−Cr2−O1′	170.8(5)
O1−Cr3−O2	169.2(3)	O2−Cr1−Cl2	82.2(2)	O2−Cr1−Cl2′	95.8(3)
O1−Cr2−Cl1	82.4(2)	O1−Cr2−Cl1′	95.9(2)	O1−Cr3−Cl1	81.8(2)
O1−Cr3−Cl2	97.0(3)	O2−Cr3−Cl1	94.8(3)	O2−Cr3−Cl2	82.4(2)
Cl2−Cr1−Cl2′	158.81(18)	Cl1−Cr2−Cl1′	158.23(18)	Cl1−Cr3−Cl2	159.16(14)
Cr1−O2−Si2	139.8(5)	Cr2−O1−Si1	136.2(5)	Cr3−O1−Si1	138.6(5)
Cr3−O2−Si2	134.8(5)	O−Si−C(av)	106.9(28)	Si−C−C(av)	110.4(79)
C−C−C(av)	108.0(29)				

tances,[14] respectively, suggest that dichromium interactions are likely to be far more significant between neighboring faces than across the box. In comparison, the average adjacent and opposite Cr···Cr distances in $[Cr(\mu\text{-}CH_2SiMe_3)_2]_4$[15] are 2.369(3) and 3.350(3) Å, respectively, because of the shorter, 3c2e dichromium−carbon bridging interactions.

3. Magnetism. The aforementioned Evans' method measurement on $[Cr(\mu\text{-}Cl)(\mu\text{-}OSi^tBu_3)]_4$ (**1**) afforded a $\mu_{eff} = 1.7\mu_B$ at 295 K, a value much lower than expected for four square-planar Cr(II) centers.[12] The possibility of extensive intermetallic interactions prompted a full temperature-dependent study (SQUID), but a ready interpretation of the magnetism remained elusive. Compound **1** displayed antiferromagnetic coupling as its μ_{eff} smoothly changed from $\sim 1.1\mu_B$ at 298 K to $\sim 0.8\mu_B$ at 180 K to $\sim 0.3\mu_B$ at 60 K, but utilization of the isotropic exchange model ($H = -J\{S_1S_2 + S_2S_3 + S_3S_4 + S_1S_4)\} = -4J(S_1S_2)$) and vector coupling scheme[16] employed by Gambarotta et al. in their investigation of $[Cr(\mu\text{-}CH_2SiMe_3)_2]_4$[15] failed to yield sensible results. It is interesting that satisfactory fits of the magnetic data collected on $[Cr(\mu\text{-}CH_2SiMe_3)_2]_4$ ($\mu_{eff} \approx 1.6\ \mu_B$ at 300 K) were obtained for $S = 1$ and $S = 2$ configurations; hence, aside from corroborating the antiferromagnetism ($J \approx -500$ cm^{-1} for both), the fits provided only minimal insight into its electronic structure. If the chromous centers in **1** were completely uncoupled, then a μ_{eff} of $9.8\mu_B$ (i.e., $\mu_{eff} = g\{(S_1(S_1+1)) + (S_2(S_2+1)) + (S_3(S_3+1)) + (S_4(S_4+1))\}^{1/2)}$) would be expected at 298 K, but this value is obviously severely attenuated.

4. Calculations on a Model Box, D_{2d} [Cr(μ-Cl)(μ-OH)] (1′). The geometry of the model tetramer [Cr(μ-Cl)(μ-OH)] (**1′**) was taken from the X-ray crystallographic coordinates of the full model $[Cr(\mu\text{-}Cl)(\mu\text{-}OSi^tBu_3)]_4$ (**1**). To facilitate the study of its electronic structure, the atomic coordinates were altered slightly to yield a D_{2d} species. UB3PW91/CEP-31G(d) calculations on **1′** were carried out on multiplicity = 17 ($S = 8$, all high-spin d^4 Cr(II) ions).[17,18]

(14) Cotton, F. A.; Walton, R. A. *Multiple Bonds Between Metal Atoms*; Oxford University Press: New York, 1993.
(15) Schulzke, C.; Enright, D.; Sugiyama, H.; LeBlanc, G.; Gambarotta, S.; Yap, G. P. A.; Thompson, L. K.; Wilson, D. R.; Duchateau, R. *Organometallics* **2002**, *21*, 3810−3816.
(16) Kambe, R. K. *J. Phys. Soc. Jpn.* **1950**, *5*, 38−43.

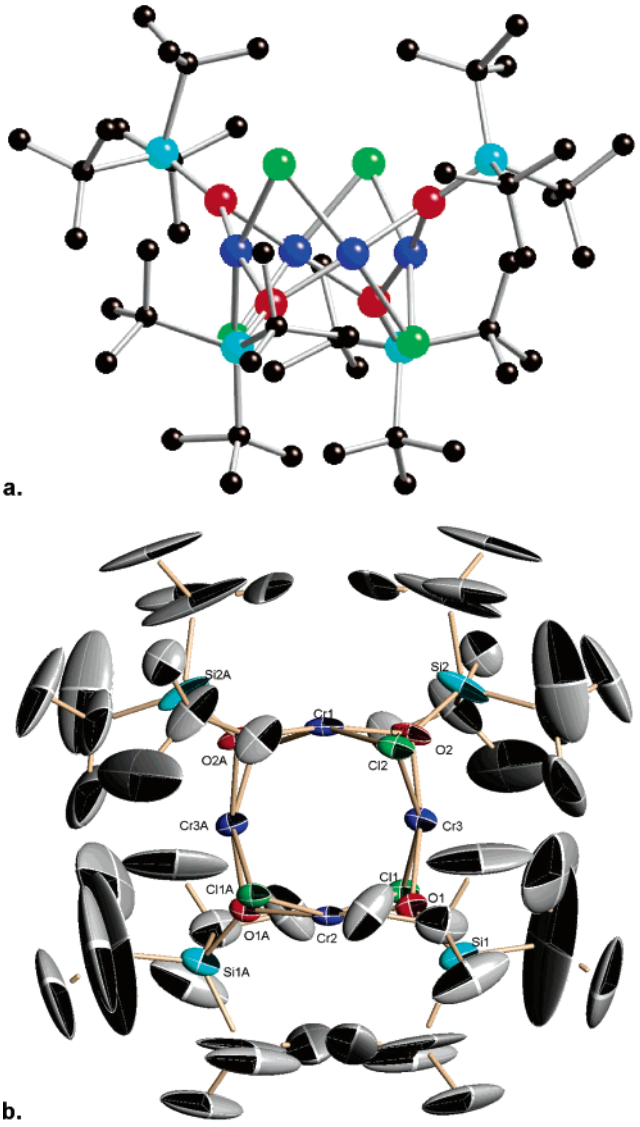

Figure 1. Molecular views of [Cr(μ-Cl)(μ-OSi^{t}Bu$_3$)]$_4$ (**1**): (a) side view revealing coplanar arrangement of Cr(II) centers in the box (dark blue = Cr, red = O, green = Cl, light blue = Si, and black = C) and (b) top view (ORTEP, 40% ellipsoids) that reveals peripheral disorder problems yet shows a well-refined core.

The 16 Cr d-based molecular orbitals illustrated in Figure 2 are within 2.1 eV. Although the d-orbital origin of some are easily discerned (−4.0007 eV is ($d_{z^2} + d_{z^2} + d_{z^2} + d_{z^2}$); −2.6953 eV is ($d_{yz} + d_{yz} + d_{yz} + d_{yz}$), etc.), extensive mixing of e-type orbitals (four sets derived from d_{z^2}, d_{xz}, d_{yz}, and $d_{x^2-y^2}$; *x* axis for each square-planar Cr is taken in the "belt" of the box) in D_{2d} renders the degenerate pairs difficult to assign. Nonetheless, it is relatively clear that the MOs in Figure 2 are grouped roughly into four σ-bonding orbitals, followed by four π-bonding orbitals, four π^* in character, and four σ-antibonding orbitals. The orbitals are similar, in terms of appearance, to those derived for [Cr(μ-CH$_2$-SiMe$_3$)$_2$]$_4$[15] by DFT methods; however, those authors chose to depict only 9 of the 16 orbitals, and yet the energy gap in those 9 orbitals spans roughly 2.5 eV. It is probably the shorter d(Cr···Cr) in [Cr(μ-CH$_2$SiMe$_3$)$_2$]$_4$ that provides the means for greater interaction in the dialkyl tetramer and a correspondingly greater spread in d-based orbitals. Although the complexity of the system obviated an assessment of its magnetism, antiferromagnetic behavior would be a logical consequence of the modest orbital splittings.

5. Box Cleavage. [Cr(μ-Cl)(μ-OSi^{t}Bu$_3$)]$_4$ (**1**) was stable in the nonpolar solvents benzene, toluene, pentane, and hexane as well as diethyl ether but was cleaved within minutes in THF to afford turquoise crystals of *trans*-(silox)-ClCr(THF)$_2$ (**2**, Scheme 1). Although its ^{1}H NMR spectrum was difficult to assign, the complex was quenched (degraded) with DCl/DOCD$_3$ to produce (silox)H/D and THF in a 1.0:2.0 ratio. Evans' method measurements[13] gave a $\mu_{eff} = 4.7\mu_B$, consistent with a high-spin chromous system. Dissolution of **2** in pentane or benzene reconstituted **1**, and thermolysis of **2** also affected the loss of THF.

When [Cr(μ-Cl)(μ-OSi^{t}Bu$_3$)]$_4$ (**1**) was exposed to 4-picoline in pentane, disproportionation accompanied deaggregation as *trans*-Cl$_2$Cr(4-pic)$_2$ and *trans*-(silox)$_2$Cr(4-pic)$_2$ (**3**) were formed. Because the former possessed limited solubility in pentane, it was easily separated via filtration, leaving an orange solution tentatively assigned as containing (silox)$_2$Cr-(4-pic)$_3$ (**3**-4-pic). Removal of the pentane and multiple triturations led to the crystallization of green rods of **3** from pentane in 97% yield. Quenching of **3** with DCl/DOCD$_3$ provided silox and 4-picoline in a 1.0:1.0 ratio, confirming the disproportionation. The ^{1}H NMR spectrum of **3** revealed the siloxide and picoline methyl protons at δ 2.54 ($\nu_{1/2} \approx$ 960 Hz) and the aromatic protons at δ 17.74 ($\nu_{1/2} \approx$ 600 Hz) and δ 54.58 ($\nu_{1/2} \approx$ 550 Hz). The μ_{eff}, as determined by Evans' method,[13] was 4.7μ_B, which is consistent with the square-planar geometry predicted for high-spin d^4 systems.

If neat 4-picoline was used to cleave **1**, then orange crystals of (silox)$_2$Cr(4-pic)$_3$ (**3**-4-pic) could be obtained. A DCl/CD$_3$-OD quench of **3**-4-pic afforded a ^{t}Bu$_3$Si:O4-pic ratio of 2:3.4; hence, **3**-4-pic was assigned the five-coordinate structure, which has precedence in the square-pyramidal chromous pyrrolyl (η^1-C$_4$H$_4$N)$_2$Cr(pyr)$_3$[19] complex reported by Gambarotta et al. 4-Picoline loss from **3**-4-pic prevented further analysis. The formation of CrCl$_2$(4-pic)$_2$[20] as a disproportionation product was confirmed by its independent synthesis from CrCl$_2$ and 4-picoline and by infrared spectroscopic comparison of the samples.

(17) Frisch, M. J.; Trucks, G. W.; Schlegel, H. B.; Scuseria, G. E.; Robb, M. A.; Cheeseman, J. R.; Zakrzewski, V. G.; Montgomery, J. A., Jr.; Stratmann, R. E.; Burant, J. C.; Dapprich, S.; Millam, J. M.; Daniels, A. D.; Kudin, K. N.; Strain, M. C.; Farkas, O.; Tomasi, J.; Barone, V.; Cossi, M.; Cammi, R.; Mennucci, B.; Pomelli, C.; Adamo, C.; Clifford, S.; Ochterski, J.; Petersson, G. A.; Ayala, P. Y.; Cui, Q.; Morokuma, K.; Malick, D. K.; Rabuck, A. D.; Raghavachari, K.; Foresman, J. B.; Cioslowski, J.; Ortiz, J. V.; Stefanov, B. B.; Liu, G.; Liashenko, A.; Piskorz, P.; Komaromi, I.; Gomperts, R.; Martin, R. L.; Fox, D. J.; Keith, T.; Al-Laham, M. A.; Peng, C. Y.; Nanayakkara, A.; Gonzalez, C.; Challacombe, M.; Gill, P. M. W.; Johnson, B. G.; Chen, W.; Wong, M. W.; Andres, J. L.; Head-Gordon, M.; Replogle, E. S.; Pople, J. A. *Gaussian 98*, revision A.1; Gaussian, Inc.: Pittsburgh, PA, 1998.
(18) (a) Hegarty, D.; Robb, M. A. *Mol. Phys.* **1979**, *38*, 1795. (b) Eade, R. H. E.; Robb, M. A. *Chem. Phys. Lett.* **1981**, *83*, 362. (c) Schlegel, H. B.; Robb, M. A. *Chem. Phys. Lett.* **1982**, *93*, 43.
(19) Edema, J. J. H.; Gambarotta, S.; Meetsma, A.; van Bolhuis, F.; Spek, A. L.; Smeets, W. J. J. *Inorg. Chem.* **1990**, *29*, 2147−2153.
(20) Holah, D. G.; Fackler, J. P. *Inorg. Chem.* **1965**, *4*, 1112−1116.

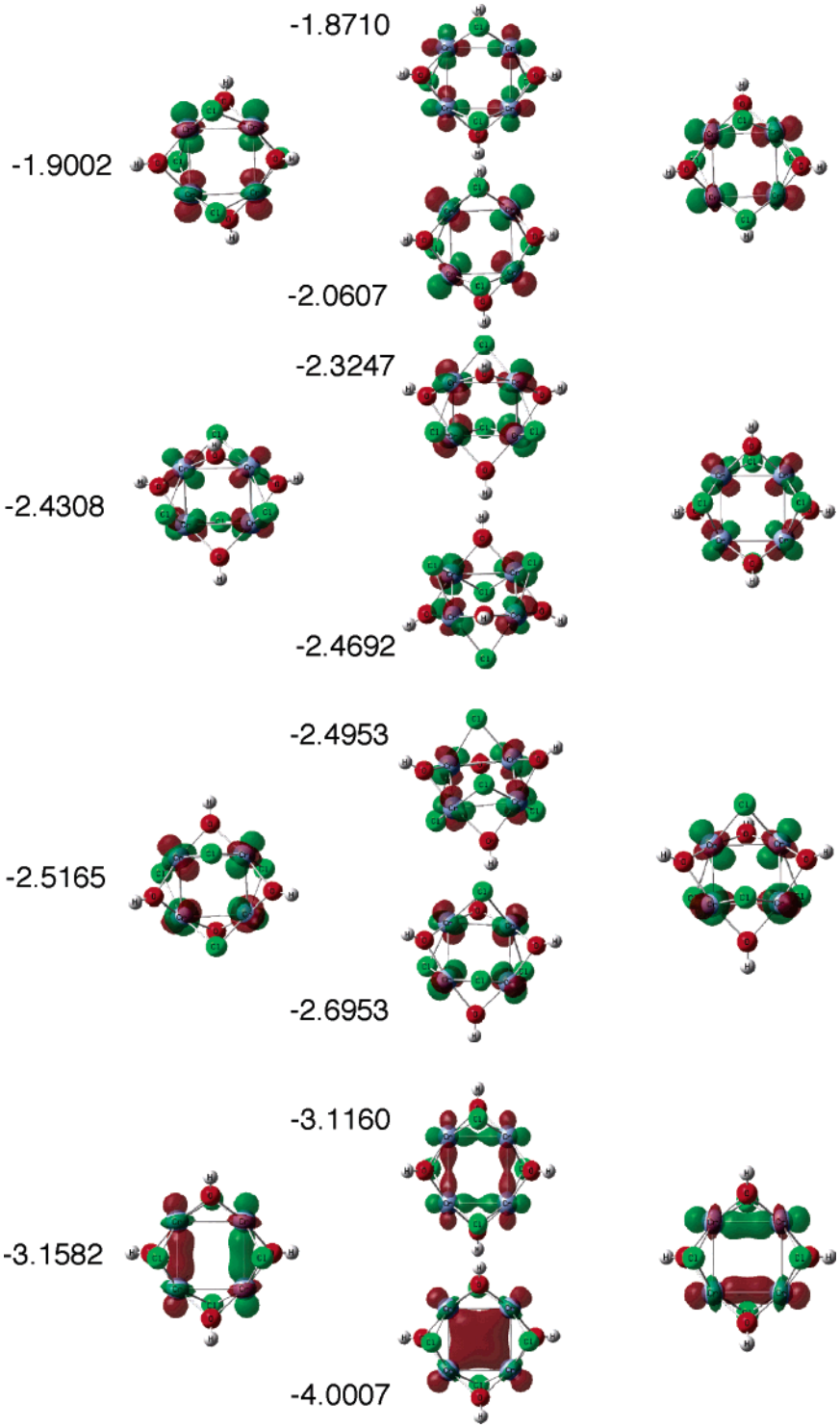

Figure 2. Sixteen Cr d-based molecular orbitals of $[Cr(\mu\text{-}Cl)(\mu\text{-}OH)]_4$ (**1′**), the model for $[Cr(\mu\text{-}Cl)(\mu\text{-}OSi^tBu_3)]_4$ (**1**). Orbital energies are in eV.

Trigonal Cr(II). 1. Synthesis of $[(^tBu_3SiO)Cr(\mu\text{-}OSi^tBu_3)_2]Na\cdot C_6H_6$ (4). When $[Cr(\mu\text{-}Cl)(\mu\text{-}OSi^tBu_3)]_4$ (**1**) was heated to 100 °C for 2.5 days in benzene in the presence of 8 equiv of Na(silox), box cleavage again occurred, and smooth conversion to powder-blue crystalline $[(^tBu_3SiO)Cr(\mu\text{-}OSi^tBu_3)_2]Na\cdot C_6H_6$ (**4**) was noted (67%, Scheme 1). The μ_{eff} of 4.8μ_B at 295 K was consistent with a high-spin trigonal Cr(II) metal center, and X-ray crystallography subsequently confirmed its general geometry. The complex appears to be one of the few three-coordinate chromous mononuclear complexes that is structurally characterized,[2] following Power's report of $[(^tBu_3CO)Cr]\{(\mu\text{-}Cl)(\mu\text{-}OC^tBu_3)Li(THF)_2\}$, which has a distorted T shape.[21]

2. Molecular Structure of $[(^tBu_3SiO)Cr(\mu\text{-}OSi^tBu_3)_2]Na(C_6H_6)$ (4). Data collection and refinement information regarding $[(^tBu_3SiO)Cr(\mu\text{-}OSi^tBu_3)_2]Na(C_6H_6)$ (**4**) is given

(21) Hvoslef, J.; Hope, H.; Murray, B. D.; Power, P. P. *J. Chem. Soc., Chem. Commun.* **1983**, 1438−1439.

Table 3. Selected Interatomic Distances (Å) and Angles (deg) for [(^{t}Bu$_3$SiO)Cr(μ-OSi^{t}Bu$_3$)$_2$]Na·C$_6$H$_6$ (**4**), [(silox)$_3$Cr][Na(dibenzo-18-crown-6)] (**5**), and (silox)$_3$Cr (**6**) and Calculated Bond Distances and Angles for [(^{t}Bu$_3$SiO)Cr(μ-OSi^{t}Bu$_3$)$_2$]Na (**4′**), [(silox)$_3$Cr]$^-$ (**5′**), and [(silox)$_3$Cr] (**6**)

	4[a]	**4′**	**5**[b]	**5′**	**6**	**6′**
Cr−O1	1.9580(16)	1.97	1.920(3), 1.891(3)	1.91	1.7786(14)	1.78
Cr−O2	1.8906(16)	1.86	1.905(3), 1.903(3)	1.91	1.7714(14)	1.78
Cr−O3	1.9719(14)	1.98	1.942(3), 1.894(3)	1.94	1.7833(14)	1.78
O1−Si1	1.6269(16)		1.598(3), 1.585(4)		1.6621(15)	
O2−Si2	1.6190(17)		1.607(3), 1.602(3)		1.6582(15)	
O3−Si3	1.6244(16)		1.605(3), 1.609(3)		1.6724(15)	
Na−O1	2.2808(19)	2.15				
Na−O3	2.2718(19)	2.12				
Cr−Na	2.9414(10)					
(Si−C)$_{av}$	1.936(8)		1.95(4), 1.945(25)		1.926(5)	
(C−C)$_{sil\ av}$	1.54(10)		1.54(4), 1.54(6)		1.541(10)	
Na−C1(O4)[c]	2.976(3)		2.647(3), 2.550(3)			
Na−C2(O5)[c]	3.058(3)		2.733(3), 2.661(4)			
Na−C3(O6)[c]	3.195(3)		2.710(4), 2.619(4)			
Na−C4(O7)[c]	3.281(3)		2.572(3), 2.581(4)			
Na−C5(O8)[c]	3.232(3)		2.652(3), 2.593(4)			
Na−C6(O9)[c]	3.068(3)		2.636(4), 2.620(3)			
O1−Cr−O2	130.95(7)	132.8	116.78(13), 118.36(16)	119.8	119.20(7)	120
O1−Cr−O3	91.28(7)	89.6	134.64(12), 129.63(16)	129.8	121.57(7)	120
O2−Cr−O3	136.17(7)	133.0	108.21(13), 111.66(16)	110.4	119.22(7)	120
Cr−O1−Si1	142.13(10)		171.66(18), 176.4(2)	161.2	162.00(10)	
Cr−O2−Si2	159.96(11)		153.25(17), 153.39(18)	151.5	163.48(10	
Cr−O3−Si3	143.36(10)		144.42(17), 155.5(2)	139.1	150.80(10)	
Na−O1−Cr	87.54(6)					
Na−O3−Cr	87.45(6)					
O1−Na−O3	76.22(6)					
Na−O1−Si1	129.99(10)					
Na−O3−Si3	128.54(9)					
(O−Si−C)$_{av}$	108.1(8)		108.8(13), 108.7(17)		106.6(8)	
(C−Si−C)$_{av}$	110.8(7)		109.7(14), 110.8(25)		112.1(6)	
(Si−C−C)$_{av}$	111.5(36)		111.4(26), 111(8)		111.5(13)	
(C−C−C)$_{av}$	107(5)		107(4), 107(4)		107.3(10)	

[a] The benzene bond distances average 1.370(14) Å and its average C−C−C angles are 120.0(10)°. [b] The two sets of data for **5** are from the two independent [(silox)$_3$Cr][Na(dibenzo-18-crown-6)] molecules; the second anion has substantial disorder in the peripheral ^{t}Bu groups. [c] The distances correspond to the *d*(Na−C(benzene)) of **4** or the *d*(Na−O(crown)) of **5**; the cation of **5** possesses $\sum$/O−Na−O = 358.4° and 360.8°, with average O−Na−O angles of 59.7(26)° and 60.1(21)°.

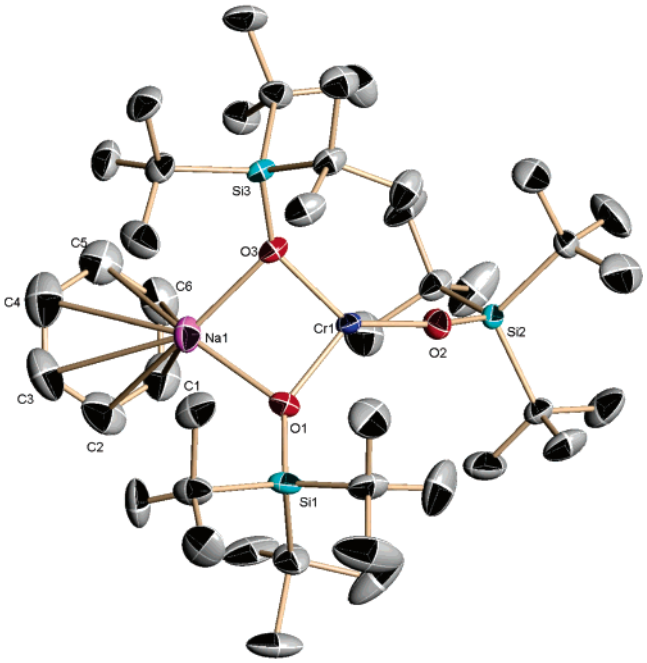

Figure 3. Molecular view (dark blue = Cr, red = O, light blue = Si, purple = Na, and black = C) of [(^{t}Bu$_3$SiO)Cr(μ-OSi^{t}Bu$_3$)$_2$]Na·C$_6$H$_6$ (**4**).

in Table 1, whereas pertinent interatomic distances and angles are given in Table 3. Figure 3 illustrates the molecular structure of **4** and reveals a rough trigonal geometry about a Cr(II) center that is distorted toward a Y shape. A d^4 trigonal molecule (^{5}E′ → (a$_2$′)^1(e″)^2(e′)^1) is expected to undergo a Jahn−Teller distortion[22−24] of some prominence because of its $d_{z^2}^1(d_{xz}d_{yz})^2(d_{x^2-y^2}, d_{xy})^1$ configuration that places one electron in the degenerate σ* orbital set, but given the nature of the bridges, it is difficult to know whether the distortion is electronically derived or simply caused by the Na(μ-OSi^{t}Bu$_3$)Cr bonding. The two bridging siloxides possess *d*(Cr−O) values of 1.9580(16) and 1.9719(14) Å, which are clearly longer than the lone terminal siloxide chromium−oxygen distance of 1.8906(16) Å. The bridging and terminal Cr−O distances are consistent with the sum of the covalent radii (1.91 Å) and reflect a lack of significant π bonding because of the partial occupation of Cr−O π* orbitals (d_{xz}, d_{yz}, $d_{x^2-y^2}$, and d_{xy} are π*) and the modest-to-poor overlap expected for the first-row transition-metal−oxygen interaction.

The μ-OSi^{t}Bu$_3$ bridges connect with the sodium cation over 2.2808(19) and 2.2718(19) Å, and these interactions cause the O1−Cr−O3 angle to be 91.28(7)°, which is considerably smaller than the 130.95(7) (O1−Cr−O2) and

(22) (a) Albright, T. A.; Burdett, J. K.; Whangbo, W.-H. *Orbital Interactions in Chemistry*; Wiley: New York, 1985. (b) Albright, T. A.; Burdett, J. K. *Problems in Molecular Orbital Theory*; Oxford University Press: New York, 1992.
(23) Alvarez, S. *Coord. Chem. Rev.* **1999**, *193*−*195*, 13−41.
(24) Bersuker, I. B. *Chem. Rev.* **2001**, *101*, 1067−1114.

136.17(7)° (O2−Cr−O3) angles that contain the terminal siloxide. The Na(O1)(O3)Cr core is bent along O1···O3 (envelope flap angle = 136.3°) so that the Na(C_6H_6) group is positioned away from the $^tBu_3Si$ groups. The Na−O distances are 2.2808(19) and 2.2718(19) Å, and the Na−O1−Si1 and Na−O3−Si3 angles are 129.99(10) and 128.54(9)°, respectively. The Cr−O1−Si1 and Cr−O3−Si3 angles are 142.13(10) and 143.36(10)°, respectively, and the terminal siloxide is bent away from the bridges, with ∠Cr−O2−Si2 = 159.96(11). These subtleties are consistent with the minimization of steric interactions about the core. Finally, the coordination sphere of the sodium cation is completed by asymmetric coordination to the benzene ring: Na1−C1, 2.976(3); Na1−C2, 3.058(3); Na1−C3, 3.195(3); Na1−C4, 3.281(3); Na1−C5, 3.232(3); Na1−C6, 3.068(3) Å.

3. Synthesis of [(silox)$_3$Cr][Na(dibenzo-18-crown-6)] (5). The question of whether the Y shape of [($^tBu_3SiO$)Cr(μ-OSi$^tBu_3$)$_2$]Na(C_6H_6) (**4**) was electronic in origin or completely dictated by its bridging ligands prompted efforts to remove the cation from the coordination sphere. Layering a benzene solution of dibenzo-18-crown-6 on a benzene solution containing 1 equiv of **4** produced baby-blue crystals of [(silox)$_3$Cr][Na(dibenzo-18-crown-6)] (**5**) in 95% yield (Scheme 1). The crystals were insoluble in nonpolar solvents, so the magnetic susceptibility was measured by SQUID magnetometry, and a μ_{eff} of 4.7μ_B was determined at 290 K. The value was consistent with a high-spin d^4 metal center with little orbital contribution;[12] hence, an X-ray crystallographic study ensued.

4. Molecular Structure of [(silox)$_3$Cr][Na(dibenzo-18-crown-6)] (5). Crystallographic details are given in Table 1, and pertinent interatomic distances and angles are given in Table 3. Figure 4 illustrates the asymmetric unit of [(silox)$_3$Cr][Na(dibenzo-18-crown-6)] (**5**) and reveals the presence of two independent cation−anion pairs. The sodium cations are sequestered by the crowns via a roughly planar complexation by their oxygen atoms, and two angularly distorted trigonal [(silox)$_3$Cr]$^-$ anions are present. The anions are shown separately in Figure 5. One O−Cr−O bond angle (∠O1−Cr1−O2 = 116.78(13), ∠O1B−Cr1B−O2B = 118.36(16)°) is roughly 120°, whereas the other two O−Cr−O bond angles may be considered to be (120 + α)° (∠O1−Cr1−O3 = 134.64(12), ∠O1B−Cr1B−O3B = 129.63(16)°) and (120 − α)° (∠O2−Cr1−O3 = 108.21(13), ∠O2B−Cr1B−O3B = 111.66(16)°). Significant distortions were not noted for the *d*(Cr−O), which are consistent with chromous−oxygen bonds as previously discussed: for Cr1 (1.922(15) Å (av), the O1, O2, and O3 distances are 1.920(3), 1.905(3), and 1.942(3) Å; for Cr1B (1.896(5) Å av), the O1B, O2B, and O3B distances are 1.891(3), 1.903(3), and 1.894(3) Å. The Cr−O−Si angles vary from 144 to 176°, but there is no justifiable correlation with bond length;[25] hence, π bonding does not appear to be an important contributor.

Trigonal Cr(III). 1. Synthesis of (silox)$_3$Cr (6). The geometric parameters associated with the pseudo-trigonal compounds above were unusual enough that a chromic analogue was prepared for comparison. Treatment of $CrCl_3(THF)_3$ with 3 equiv of $NaOSi^tBu_3$ in THF at 60 °C for 18 h afforded emerald-green (silox)$_3$Cr (**6**, 65%) upon crystallization (eq 1).

$$CrCl_3(THF)_3 + 3NaOSi^tBu_3 \xrightarrow[THF,\ -3NaCl]{60\ °C,\ 18\ h} \underset{\mathbf{6}}{(silox)_3Cr} \quad (1)$$

A trigonal chromic derivative is expected to possess a nondegenerate ($^3A_2'$) ground state and would not be subject to Jahn−Teller distortion.[22−24]

2. Molecular Structure of (silox)$_3$Cr (6). Details of the crystallographic study pertaining to (silox)$_3$Cr (**6**) are given in Table 1, and a list of its geometric parameters is given in Table 3. Figure 6 illustrates the nearly ideal trigonal-planar environment of **6**, which possesses O−Cr−O angles of 119.20(7), 121.57(7), and 119.22(7)° and an average *d*(Cr−O) of 1.778(6) Å. This Cr(III) distance is well below the average Cr(II)−O distance in the anions of **5** (1.909(19) Å), and the difference (0.131 Å) is much greater than that predicted from ionic radii (Δd = 0.0185 Å). The anionic character of **5** and the occupation of a σ^* orbital are the dominant factors responsible for the lengthening of its *d*(Cr−O)'s relative to those of neutral **6**. It is also possible that some minimal π bonding is now present, despite the contraction of the d orbitals in the higher oxidation state.

Calculational Models [($^tBu_3SiO$)Cr(μ-OSi$^tBu_3$)$_2$]Na (4′) and [(silox)$_3$Cr]$^-$ (5′). Preliminary calculations were done to investigate the ground-state multiplicity of Cr(silox)$_3^-$ (**5′**). Starting from the same trigonal-planar (∠O−Cr−O = 120°) geometry, **5′** was optimized for both triplet and quintet spin states using QM/MM methods.[17,26−28] The ground state was predicted to be the quintet (E(^{5}E′) < E(^{3}E′) by 29.2 kcal/mol) according to the QM/MM calculations, which is consistent with the experimental magnetic moment that reflects the relatively weak field of the siloxides. The quintet state was also used in the calculations on [($^tBu_3SiO$)Cr(μ-OSi$^tBu_3$)$_2$]Na (**4′**).

Frontier orbital considerations lead one to expect that a trigonal-planar, high-spin d^4 MX_3 complex will be subject to Jahn−Teller distortion as a consequence of its orbitally degenerate ground state.[22−24] Although a trigonal-planar coordination geometry (albeit very slightly distorted from perfect 3-fold symmetry) was used to start the calculations on Cr(silox)$_3^-$, a distorted trigonal-planar species was obtained upon geometry optimization, which is consistent with a Jahn−Teller distortion of the HS d^4 Cr^{II}. The frontier molecular orbitals of Cr(silox)$_3^-$ (**5′**) show the following splitting: E(d_{z^2}) < E(d_{xz}) ≈ E(d_{yz}) < E(d_{xy}) < E($d_{x^2-y^2}$). The position of d_{z^2} below the $d_{xz}d_{yz}$ pair is a result of modest π donation from the oxygen atoms of the silox ligands, and

(25) Steffey, B. D.; Fanwick, P. E.; Rothwell, I. P. *Polyhedron* **1990**, *9*, 963−968.

(26) (a) Becke, A. D. *J. Chem. Phys.* **1993**, *98*, 5648. (b) Burke, K.; Perdew, J. P.; Wang, Y. In *Electronic Density Functional Theory: Recent Progress and New Directions*; Dobson, J. F., Vignale, G., Das, M. P., Eds.; Plenum: New York, 1998.

(27) Vreven, T.; Morokuma, K. *J. Comput. Chem.* **2000**, *21*, 1419−1432.

(28) Rappé, A. K.; Casewit, C. J.; Colwell, K. S.; Goddard, K. S., III; Skiff, W. M. *J. Am. Chem. Soc.* **1992**, *114*, 10024−10035.

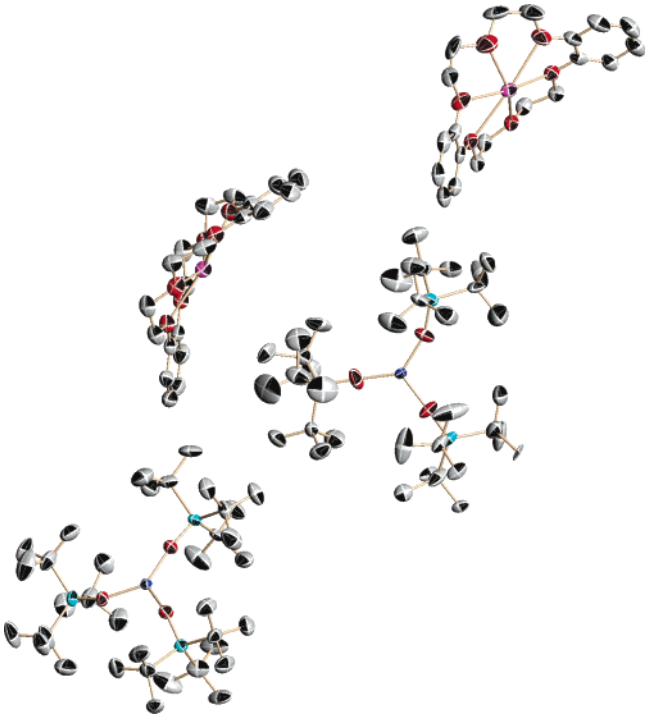

Figure 4. View of the asymmetric unit (dark blue = Cr, red = O, light blue = Si, purple = Na, and black = C) of [(silox)$_3$Cr][Na(dibenzo-18-crown-6)] (**5**); solvent molecules have been excluded.

the $d_{xy}d_{x^2-y^2}$ pair, which is degenerate in trigonal-planar geometry, has now split because of the Jahn−Teller distortion, as Figure 7 illustrates. The $E(d_{x^2-y^2}) - E(d_{xy})$ orbital gap does not truly reflect the transition energy, particularly in light of possible inaccuracies in the evaluation of Kohn−Sham virtual orbital energies.[29] Complete active space SCF (CASSCF) calculations with a minimal active space composed of the five Cr 3d orbitals and the four electrons contained therein suggest a $d_{xy} \rightarrow d_{x^2-y^2}$ transition energy of 0.3 eV.

The distortion is certainly "real" because optimization of neutral Cr(silox)$_3$ (**6′**) at the same theory level (quartet spin state) starting from the anion geometry in Figure 8 reverts to trigonal-planar geometry (Cr−O = 1.78, SiO = 1.73 Å; Cr−O−Si = 166−173, O−Cr−O = 120°), as observed in the experimental structure. As Table 3 shows, the calculated O−Cr−O angles of Cr(silox)$_3^-$ (**5′**, 120, (120 + α), and (120 − α)°; α ≈ 10°) are in excellent agreement with experimental values for the two independent molecules in the asymmetric unit cell of [(silox)$_3$Cr][Na(dibenzo-18-crown-6)] (**5**).

A greater distortion from ideal trigonal planar might be expected a priori because crystal-field arguments suggest a strong driving force for the trigonal-planar to T-shape distortion.[23] It is plausible that the small angular distortion observed experimentally and computationally is a consequence of the steric bulk of the silox ligands. For example, UB3PW91/6-31G (same level of theory)[26] geometry optimization of quintet Cr(OH)$_3^-$ revealed a subtly pyramidalized, T-shaped anion with O−Cr−O angles of 90, 90, and 168°, but a second, planar Y-shaped species with O−Cr−O angles of 96, 132, and 132° was found to be ∼20 kcal/mol lower in energy. Regardless, both optimizations support the contention that distortion from trigonal-planar geometry is sensitive to steric factors because the observed Cr(silox)$_3^-$ is asymmetric with respect to the T or Y shapes that are the electronically preferred structures for HS d^4 Cr(II). In-plane distortions of three-coordinate complexes from trigonal-planar to T and Y shapes are quite facile,[30] and thus it seems reasonable to presume that they will be quite sensitive to the steric influence of the bulky silox ligands in the present case.

Ligating Na^+ to the anion, followed by QM/MM geometry optimization, causes further distortion of the chromium inner coordination sphere. As Table 3 and Figure 8 reveal, the calculated structure for [(^{t}Bu$_3$SiO)Cr(μ-OSi^{t}Bu$_3$)$_2$]Na (**4′**) is remarkably close to that of [(^{t}Bu$_3$SiO)Cr(μ-OSi^{t}Bu$_3$)$_2$]Na-(C$_6$H$_6$) (**4**). Calculated chromium−oxygen distances are within 0.03 Å of those determined for **4**, and the O−Cr−O angles are within 3° of those of the experimental structure, despite the removal of the weakly bound benzene that ligates the sodium cation. Finally, the calculated Si−O bond lengths are about 0.1 Å longer (as they are in **5′** and **6′**) than the experimentally determined values, and this artificial increase may have caused an underestimation of the steric impact of the ^{t}Bu$_3$SiO groups on the calculated geometry, resulting in some low bond angles.

Discussion

[Cr(μ-Cl)(μ-OSi^{t}Bu$_3$)]$_4$ (1). 1. Aggregation of "(^{t}Bu$_3$SiO)-CrCl". This initial foray into studying the aggregation of [(^{t}Bu$_3$SiO)MX]$_n$ successfully led to the preparation of the intriguing "chromous box", [Cr(μ-Cl)(μ-OSi^{t}Bu$_3$)]$_4$ (**1**), an unusual example of a cluster based on a square-planar motif.[31−35] The tetranuclear chromous complex could be deaggregated with simple donors, and square-planar Cr(II) complexes were the products of box cleavage. In the case of THF, the formation of *trans*-(silox)CrCl(THF)$_2$ (**2**) was reversible because **1** could be reconstituted upon thermolysis of **2** or its dissolution in pentane. With 4-picoline, disproportionation accompanied box scission, and with both donor solvents, the products are best construed as square-planar derivatives, although no structural studies on these simple molecules were carried out. Four-coordinate, high-spin Cr(II)

(29) Williams, H. L.; Chabalowski, C. F. *J. Phys. Chem. A* **2001**, *105*, 646−659.

(30) Komiya, S.; Albright, T. A.; Hoffmann, R.; Kochi, J. K. *J. Am. Chem. Soc.* **1976**, *98*, 7255−7265.

(31) (a) [Ni(μ-*N*-methylpiperidine-4-thiolato)$_2$]$_4$: Gaete, W.; Ros, J.; Solans, X.; Font-Altaba, M.; Briansó, J. L. *Inorg. Chem.* **1984**, *23*, 39−43. (b) [Ni(μ-SC$_6$H$_{11}$)$_2$]$_4$: Kriege, M.; Henkel, G. *Z. Naturforsch.* **1987**, *42b*, 1121−1128. (c) [Ni(μ-SC$_3$H$_7$)$_2$]$_4$: Krüger, T.; Krebs, B.; Henkel, G. *Angew. Chem., Int. Ed. Engl.* **1989**, *1*, 61−62.

(32) (a) [Ni(μ-SEt)$_2$]$_5$: Kriege, M.; Henkel, G. *Z. Naturforsch.* **1987**, *42b*, 1121−1128. (b) [Ni(μ-SCH$_2$SiMe$_3$)$_2$]$_5$: Koo, B.-K.; Block, E.; Kang, H.; Liu, S.; Zubieta, J. *Polyhedron* **1988**, *7*, 1397−1399.

(33) (a) [Ni(μ-SEt)$_2$]$_6$: Woodward, P.; Dahl, L. F.; Abel, E. W.; Crosse, B. C. *J. Am. Chem. Soc.* **1965**, *87*, 5251−5253. (b) Gould, R. O.; Harding, M. M. *J. Chem. Soc. A* **1970**, 875−881.

(34) [Ni(μ-SCH$_2$CO$_2$Et)$_2$]$_8$: Dance, I. G.; Scudder, M. L.; Secomb, R. *Inorg. Chem.* **1985**, *24*, 1201−1208.

(35) Dance, I. G. *Polyhedron* **1986**, *5*, 1037−1104.

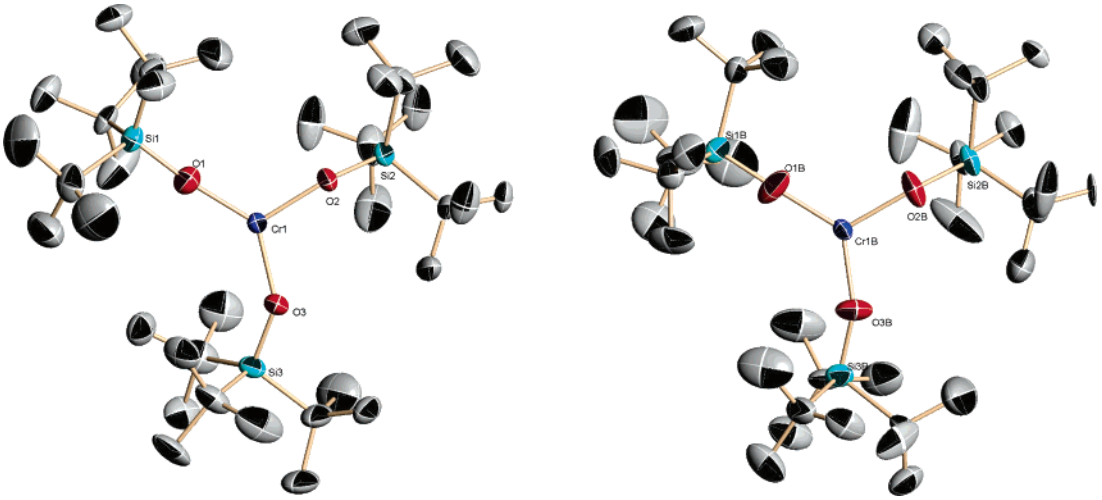

Figure 5. Molecular view (dark blue = Cr, red = O, light blue = Si, and black = C) of the two independent $[(silox)_3Cr]^-$ anions of $[(silox)_3Cr][Na(dibenzo\text{-}18\text{-}crown\text{-}6)]$ (**5**).

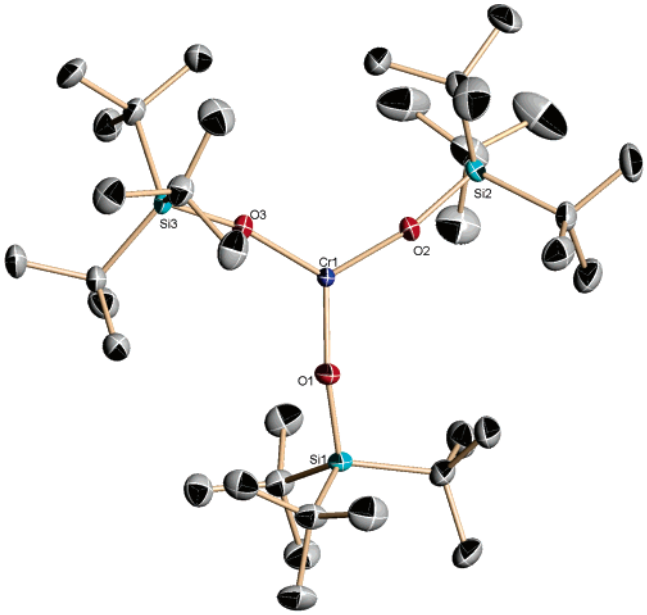

Figure 6. Molecular view (dark blue = Cr, red = O, light blue = Si, and black = C) of $(silox)_3Cr$ (**6**).

complexes have a decided electronic preference for square-planar geometry, and there are numerous examples including *trans*-$Cr(OSi(O^tBu)_3)_2(NHEt_2)_2$,[36] *trans*-$Cr(O\text{-}2,6\text{-}^tBu_2C_6H_2\text{-}4\text{-}Me)_2(THF)_2$,[37] $[(TMEDA)Na]_2Cr(O\text{-}2,6\text{-}Me_2C_6H_3)_4$,[38] *trans*-$Cr(NPh_2)_2(pyr)_2$,[39] $[Na(THF)_2]_2Cr(NPh_2)_4$,[39] and *trans*-$Cr(CH_2CMe_3)_2(PMe_3)_2$.[40]

2. Electronics and Computation. Despite intensive computational efforts, only modest insight into the electronic coupling of the four square-planar chromous centers in **1** and its curious antiferromagnetic behavior was obtained because of the complicated nature of the system. The density of states in this weakly coupled tetranuclear complex prohibits a detailed look at their scope and energetics, which is necessary to describe a property such as magnetic behavior. Nonetheless, the critical molecular orbitals of the Cr_4 core are reminescent of those calculated by Gambarotta et al. for the related tetranuclear $[Cr(\mu\text{-}CH_2SiMe_3)_2]_4$.[15] In comparison, the MO orbital energy differences of **1** are more subtle, which is consistent with a less interactive system.

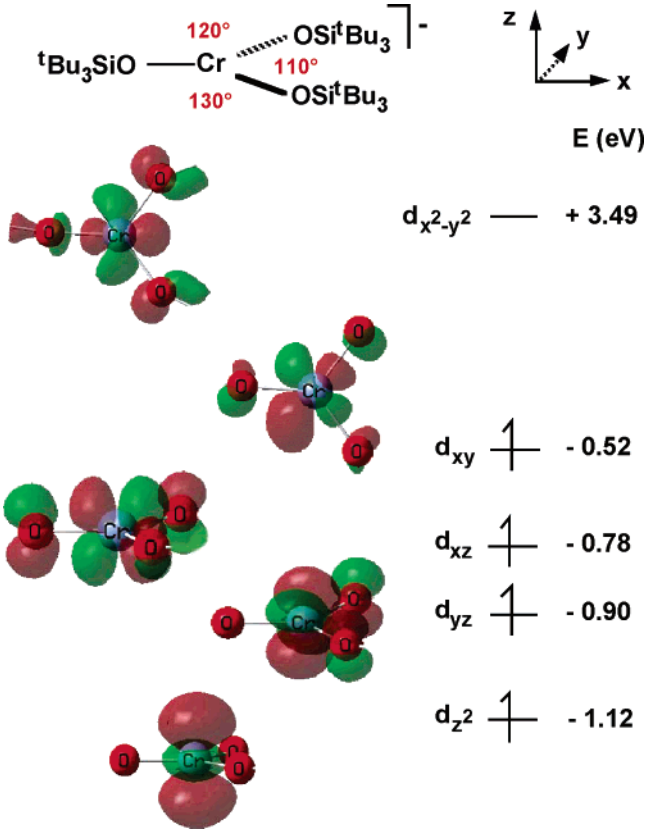

Figure 7. Frontier molecular orbitals of HS-d^4-$Cr(silox)_3^-$ (**5′**), the anion of $[(silox)_3Cr][Na(dibenzo\text{-}18\text{-}crown\text{-}6)]$ (**5**). Si^tBu_3 groups were removed for clarity. Orbital energies were calculated at UB3PW91/6-31G level of theory.

(36) Terry, K. W.; Gantzel, P. K.; Tilley, T. D. *Inorg. Chem.* **1993**, *32*, 5402−5404.
(37) Edema, J. J. H.; Gambarotta, S.; van Bolhuis, F.; Smeets, W. J. J.; Spek, A. L. *Inorg. Chem.* **1989**, *28*, 1407−1410.
(38) Edema, J. J. H.; Gambarotta, S.; van Bolhuis, F. Spek, A. L. *J. Am. Chem. Soc.* **1989**, *111*, 2142−2147.
(39) Edema, J. J. H.; Gambarotta, S.; Meetsma, A.; Spek, A. L.; Smeets, W. J. J.; Chiang, M. Y. *J. Chem. Soc., Dalton Trans.* **1993**, 789−797.
(40) Hermes, A. R.; Morris, R. J.; Girolami, G. S. *Organometallics* **1988**, *7*, 2372−2379.

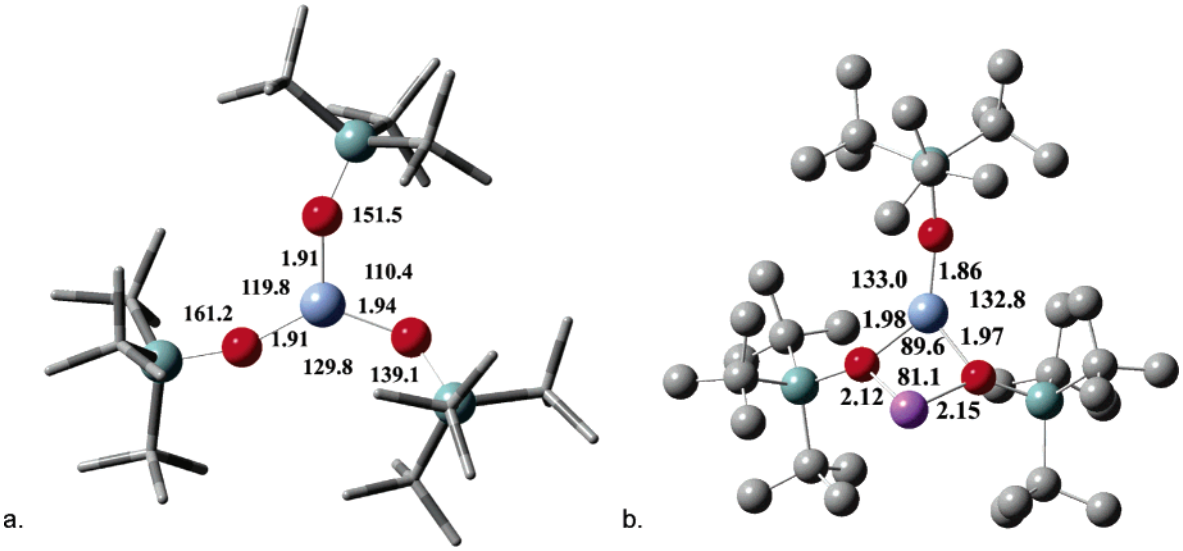

Figure 8. Calculated QM/MM geometries: (a) the $Cr(silox)_3^-$ anion (**5′**) of $[(silox)_3Cr][Na(dibenzo\text{-}18\text{-}crown\text{-}6)]$ (**5**) and (b) $NaCr(silox)_3$ (**4′**), the model for $[(^tBu_3SiO)Cr(\mu\text{-}OSi^tBu_3)_2]Na(C_6H_6)$ (**4**) sans benzene.

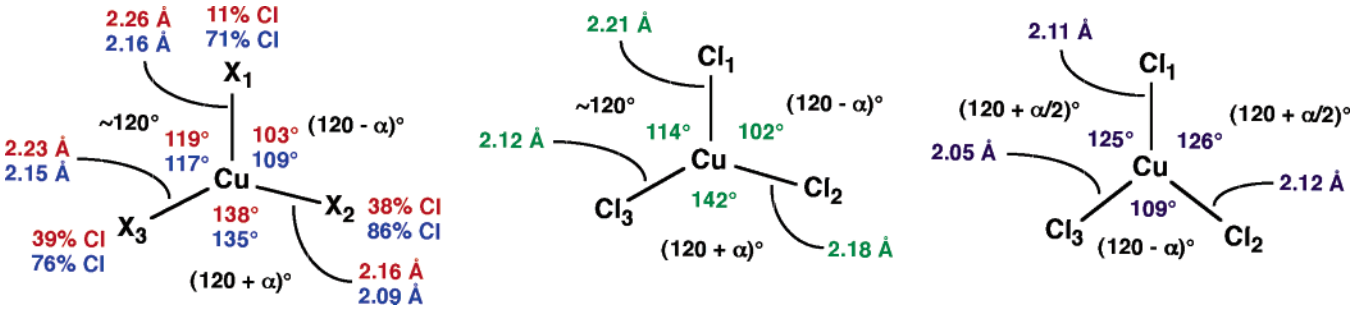

Figure 9. Metric parameters for $[Ph_3NPPh_3]^+[CuCl_{0.9}Br_{2.1}]^-$, $[Ph_3PNPPh_3]^+[CuCl_{2.4}Br_{0.6}]^-$, and $[CuCl_3]^-$.

Distorted Trigonal $[(silox)_3Cr]^-$. A trigonal high-spin d^4 center ($^5E'$) will undergo a Jahn−Teller distortion to what theory portrays as either a T-shaped or Y-shaped complex.[22−24] For the $[(silox)_3Cr]^-$ anion of $[(silox)_3Cr][Na(dibenzo\text{-}18\text{-}crown\text{-}6)]$ (**5**), the ultimate distortion was neither. Instead, the complex manifested a set of 120, $(120 - \alpha)°$, and $(120 + \alpha)°$ angles (where $\alpha \approx 10°$) that seemed to suggest the presence of a second-order perturbation.[24] The corresponding computational studies agreed with previous efforts when $(HO)_3Cr^-$ was calculated, but inclusion of the silox groups via molecular mechanics provided a computation model, $(silox)_3Cr^-$ (**5′**), that essentially matched the experimentally observed structure. For a trigonal $(silox)_3M$ species in C_{3h} symmetry, a T- or Y-shaped distortion should be sterically possible; hence, the influences that drive the ground state to its less symmetric form are not readily discerned. If one views the free anions depicted in Figure 4, then it is notable that Cr−O1−Si1 is nearly linear, whereas Cr−O2−Si2 is bent but out of the O_3Cr plane. Cr−O3−Si3 is bent in the plane, and the silox bulk is directed toward the $(120 + \alpha)°$ angle. It appears that bent Cr−O−Si linkages are best accommodated out of the O_3Cr plane, but the electronic distortion allows one silox group to bend in plane. The remaining angles then adjust to this perturbation. When the Na^+ is present in $[(^tBu_3SiO)Cr(\mu\text{-}OSi^tBu_3)_2]Na(C_6H_6)$ (**4**), the distortion toward a Y shape is so pronounced, because of direct binding with the cation, that secondary steric effects are not consequential in either the experimental or calculational structures.

It is interesting that other trigonal complexes that are subject to Jahn−Teller effects also exhibit asymmetric distortions. Dance and co-workers successfully synthesized and isolated two Cu^{II} complexes, $[Ph_3NPPh_3]^+[CuCl_{0.9}Br_{2.1}]^-$ and $[Ph_3PNPPh_3]^+[CuCl_{2.4}Br_{0.6}]^-$, which serve as examples of distorted three-coordinate d^9 complexes.[41] Figure 9 shows the metric parameters for the two species, which exhibit ~120, $(120 + \alpha)$, and $(120 - \alpha)°$ angles and a long bond opposite the widest angle. In a search of the Cambridge structural database, Dance also uncovered a spectator $[CuCl_3]^-$ anion to the lanthanide cation $[GdCl_2(OPPh_3)_4]^+$ that also possesses a related asymmetric geometry.[42] Curiously, another spectator $[CuCl_3]^-$ anion present exhibits a simple Y-shaped distortion. It is conceivable that secondary electronic effects (e.g., mixing of excited-state configurations) may be playing a role in the asymmetric distortion, but it is more likely that T- or Y-shaped molecules exist in shallow potential-energy wells whereby modest steric or intermolecular interactions can perturb the geometry with minimal changes in the overall energy.

Three-coordinate high-spin d^4 systems are rarely observed because they are reactive electronically unsaturated species

(41) Hasselgren, C.; Jagner, S.; Dance, I. *Chem.—Eur. J.* **2002**, *8*, 1269−1278.
(42) Xukun, W.; Mingjie, Z.; Jitao, W. *Jiegou Huaxue* **1988**, *7*, 142−147.

that must be stabilized by sterically bulky ligands. One rare example of a monomeric homoleptic three-coordinate high-spin d^4 molecule is $Mn(N(SiMe_3)_2)_3$.[43] This molecule is perfectly trigonal planar because the manganese atom sits on a crystallographically imposed 3-fold axis. Mn^{III} should be subject to a significant Jahn−Teller distortion for the reasons discussed above, but the effect may not have been observed because of the steric bulk of the $-N(TMS)_2$ groups or for crystallographic reasons; 3-fold disorders can mask subtle distortions.

Trigonal (silox)$_3$Cr (6). Structurally characterized three-coordinate chromic compounds are rare, but there are a few examples:[2] the slightly pyramidal $Cr[CH(SiMe_3)_2]_3$[44,45] and the trigonal-planar chromic amides $Cr(NRR')_3$ (R,R′ = ^{i}Pr;[46] R,R′ = $SiMe_3$;[47] R = $C(CD_3)_2Me$, R′ = 3,5-$C_6H_3Me_2$).[48] Other less-well-characterized chromic complexes formulated as three-coordinate species include $Cr\{OSiMe_2[C(SiMe_3)_3]\}_3$,[49] $Cr(PCy_2)_3$,[50] $Cr(NRR')_3$ (R = $C(CD_3)_2Me$, R′ = 2,5-C_6H_3-FMe),[51] and chromium(III) trimesityl.[52]

Conclusions

Generation of $[Cr(\mu\text{-Cl})(\mu\text{-OSi}^t\text{Bu}_3)]_4$ (**1**) revealed that the aggregation of "(silox)CrCl" could be controlled to a certain extent and suggests that continuing studies of (silox)MX will lead to a variety of $[(silox)MX]_n$ species akin to those derived from "(^{t}Bu$_3$SiS)MX".[10,11] The smaller d(M−O) relative to d(M−S) will probably lead to clusters rather than oligomeric species. The tetrameric box served as a valuable starting material for $[(silox)_3Cr]^-$, which exhibits an asymmetric distortion from trigonal symmetry that is derived from a Jahn−Teller effect and steric influences. Its X-ray crystal structure is the first of the tris-silox genre of compounds.

Experimental Section

General Considerations. All of the manipulations were performed using either glovebox or high vacuum line techniques. Hydrocarbon solvents containing 1−2 mL of added tetraglyme and ethereal solvents were distilled under nitrogen from purple sodium benzophenone ketyl and vacuum transferred from the same prior to use. Benzene-d_6 was dried over activated 4-Å molecular sieves, vacuum transferred, and stored under N_2; THF-d_8 was dried over sodium benzophenone ketyl. All of the glassware was oven dried, and NMR tubes for sealed-tube experiments were flame dried under dynamic vacuum also. Na(silox)[3] and $Cl_2Cr(THF)_2$[53] were prepared via literature methods.

NMR spectra were obtained using Varian XL-400, INOVA-400, and Unity-500 spectrometers, and chemical shifts are reported relative to benzene-d_6 (^{1}H, δ 7.15; ^{13}C{^{1}H}, δ 128.39) and THF-d_8 (^{1}H, δ 3.58; ^{13}C, δ 67.57). Infrared spectra were recorded on a Nicolet Impact 410 spectrophotometer interfaced to a Gateway PC. Elemental analyses were performed by Oneida Research Services, Whitesboro, NY, or Robertson Microlit Laboratories, Madison, NJ. Magnetic moments were determined in C_6D_6 at room temperature using Evans' method[13] with an applied diamagnetic correction. Variable-temperature magnetic susceptibility measurements were performed on a Quantum Design SQUID magnetometer equipped with a 7-T magnet. Pascal's constants were used to estimate the diamagnetic correction that was subtracted from the experimental susceptibility, yielding the molar susceptibility.

Procedures. 1. $[Cr(\mu\text{-Cl})(\mu\text{-OSi}^t\text{Bu}_3)]_4$ (1). A 50-mL flask was charged with $CrCl_2(THF)_2$ (0.882 g, 3.302 mmol), $NaOSi^tBu_3$ (0.786 g, 3.296 mmol), and THF (30 mL). The mixture was stirred at 23 °C for 18 h, and the solvent was removed to yield a turquoise solid. The solid was heated at 79 °C under vacuum for 45 min to give a purple solid that was extracted into benzene and filtered. After slow evaporation of the solvent (3 days), dark-purple rods formed (0.780 g, 78%). ^{1}H NMR (C_6H_6, 400 MHz): δ 1.42 ($\nu_{1/2} \approx$ 270 Hz). IR (Nujol mull, NaCl, cm^{-1}): 1193 (w), 1011 (m), 933 (m), 820 (s), 722 (w), 626 (s). UV−vis (benzene; λ_{max}, nm (ϵ, M^{-1}cm^{-1})): 529 (270), 612 (260). Anal. Calcd for $C_{12}H_{27}$-OSiClCr: C, 47.58; H, 9.00; Cl, 11.70. Found: C, 47.4; H, 9.1; Cl, 11.7. $\mu_{eff}(Cr_4) = 1.7\mu_B$ at 295 K (Evans' method in C_6D_6).

2. *trans*-(^{t}Bu$_3$SiO)CrCl(THF)$_2$ (2). A 10-mL flask was charged with **1** (0.075 g, 0.062 mmol) and THF (4 mL). The solution was stirred overnight, and the solvent was removed by slow evaporation, yielding turquoise crystals of the product quantitatively. ^{1}H NMR (THF-d_8, 400 MHz): resonances too broad to identify. IR (Nujol mull, NaCl, cm^{-1}): 1294 (w), 1245 (w), 1193 (m), 1181 (m), 1035 (s), 998 (s), 932 (m), 889 (s), 818 (s), 615 (s). UV−vis (benzene; λ_{max}, nm (ϵ, M^{-1}cm^{-1})): 814 (60). Anal. Calcd for $C_{16}H_{35}O_2SiClCr$ (desolvated): C, 51.24; H, 9.43; Cl, 9.45. Found: C, 51.5; H, 9.4; Cl, 9.5. $\mu_{eff} = 4.7\mu_B$ at 295 K (Evan's method in THF-δ_8). A quench with DCl/CD_3OD afforded silox/THF = 1.0:2.0 by ^{1}H NMR spectroscopic analysis.

3. *trans*-(^{t}Bu$_3$SiO)$_2$Cr(4-pic)$_2$ (3). A 10-mL flask was charged with $[Cr(\mu\text{-Cl})(\mu\text{-OSi}^t\text{Bu}_3)]_4$ (**1**, 0.300 g, 0.248 mmol), 4-picoline (2 mL), and pentane (10 mL). The mixture was stirred for 1 h, and the solvent was removed under vacuum. The orange solid was triturated twice with pentane and filtered. Slow evaporation of the pentane yielded the product as green rods (0.320 g, 97% based on ^{t}BuSiO). ^{1}H NMR (C_6H_6, 400 MHz): δ 54.58 ($\nu_{1/2} \approx$ 550 Hz) 4H (=CH−), 17.74 ($\nu_{1/2} \approx$ 600 Hz) 4H (=CH−), 2.54 ($\nu_{1/2} \approx$ 960 Hz) 60 H (^{t}Bu, Me). IR (Nujol mull, NaCl, cm^{-1}): 1620 (s), 1500 (w), 1223 (w), 1209 (w), 995 (s), 965 (s), 932 (m), 814 (s), 723 (w), 613 (s). Anal. Calcd for $C_{36}H_{68}N_2O_2Si_2Cr$: C, 64.60; H, 10.26; N, 4.19. Found: C, 63.7; H, 9.9; N, 3.9. $\mu_{eff} = 4.7\mu_B$ at 295 K (Evans' method in C_6D_6). A quench with DCl/CD_3OD afforded silox/4-pic = 1.0:1.0 by ^{1}H NMR spectroscopic analysis.

4. [(^{t}Bu$_3$SiO)Cr(μ-OSi^{t}Bu$_3$)$_2$]Na·C$_6$H$_6$ (4). A 10-mm o.d. glass tube was charged with **1** (0.300 g, 0.248 mmol), $NaOSi^tBu_3$ (0.473 g, 1.983 mmol), and 8 mL of benzene. The tube was degassed, sealed, and heated at 100 °C for 2.5 days. The baby-blue solution was filtered, and the solvent was removed to yield 529 mg of blue crystalline **4** (67%). ^{1}H NMR (C_6H_6, 400 MHz): δ 2.27 ppm ($\nu_{1/2} \approx$ 1100 Hz). IR (Nujol mull, NaCl, cm^{-1}): 1255 (w), 1128 (w), 1012 (w), 972 (m), 926 (s), 908 (s), 819 (s), 698 (m), 618 (s). UV−vis (THF; λ_{max}, nm (ϵ, M^{-1}cm^{-1})); 751 (90). Anal. Calcd for

(43) Ellison, J. J.; Power, P. P.; Shoner, S. C. *J. Am. Chem. Soc.* **1989**, *111*, 8044−8046.
(44) Barker, G. K.; Lappert, M. F. *J. Organomet. Chem.* **1974**, *76*, C45−C46.
(45) Barker, G. K.; Lappert, M. F.; Howard, J. A. K. *J. Chem. Soc., Dalton. Trans.* **1978**, 734−740.
(46) Bradley, D. C.; Hursthouse, M. B.; Newing, C. W. *J. Chem. Soc., Chem. Commun.* **1971**, 411.
(47) Köhn, R. D.; Kociok-Köhn, G.; Haufe, M. *Chem. Ber.* **1996**, *129*, 25−27.
(48) Odom, A. L.; Cummins, C. C.; Protasiewicz, J. D. *J. Am. Chem. Soc.* **1995**, *117*, 6613−6614.
(49) Blanchard, H.; Hursthouse, M. B.; Sullivan, A. C. *J. Organomet. Chem.* **1988**, *341*, 367−371.
(50) Issleib, K.; Wenschuh, E. *Chem. Ber.* **1964**, *97*, 715−720.
(51) Stokes, S. L.; Davis, W. M.; Odom, A. L.; Cummins, C. C. *Organometallics* **1996**, *15*, 4521−4530.
(52) Stolze, G. *J. Organomet. Chem.* **1966**, *6*, 383−388.
(53) Kern, R. J. *Inorg. Nucl. Chem.* **1962**, *24*, 1105−1109.

$C_{36}H_{81}O_3Si_3NaCr$ (desolvated): C, 59.93; H, 11.34. Found: C, 60.1; H, 11.7. $\mu_{eff} = 4.8\mu_B$ at 295 K (Evan's method in C_6D_6).

5. [(^{t}Bu$_3$SiO)$_3$Cr][Na(dibenzo-18-crown-6)] (5). Dibenzo-18-crown-6 (0.046 g, 0.128 mmol) was added to a benzene (3 mL) solution of [(^{t}Bu$_3$SiO)Cr(μ-OSi^{t}Bu$_3$)$_2$]Na·C_6H_6 (**4**) (0.100 g, 0.125 mmol) in a 4-dram vial. Baby-blue crystals of the product formed over 12 h in near-quantitative yield (95%). Low solubility prevented NMR spectroscopic analysis. IR (Nujol mull, NaCl, cm^{-1}): 1601 (s), 1328 (m), 1256 (s), 1213 (s), 1128 (s), 1073 (m), 968 (s), 819 (s), 779 (m), 738 (s), 615 (s). Anal. Calcd for $C_{56}H_{105}O_9Si_3NaCr$: C, 62.17; H 9.80. Found: C, 62.7; H 9.4. $\mu_{eff} = 4.7\mu_B$ at 295 K, SQUID.

6. (^{t}Bu$_3$SiO)$_3$Cr (6). A 50-mL bomb was charged with NaOSi^{t}Bu$_3$ (0.501 g, 2.101 mmol), $CrCl_3(THF)_3$ (0.262 g, 0.699 mmol), and THF (20 mL). The solution was heated at 60 °C for 18 h. The solvent was removed, and the solid was triturated with pentane three times, extracted into pentane, and filtered. The green solution was concentrated and cooled to −78 °C, yielding a green crystalline product (0.319 g, 65%). ^{1}H NMR (C_6D_6): d 2.39 ppm ($\nu_{1/2} \approx 360$ Hz). IR (Nujol mull, NaCl, cm^{-1}): 1188 (w), 1154 (w), 1100 (m), 1060 (m), 1012 (m), 931 (s), 881 (bs), 819 (s), 793 (m), 623 (s). Anal. Calcd for $C_{36}H_{81}O_3Si_3Cr$: C, 61.9; H, 11.6. Found: C, 60.8; H, 11.7. $\mu_{eff} = 3.7\mu_B$ at 295 K (Evans' method in C_6D_6).

X-ray Crystal Structure Determinations. 7. [Cr(μ-Cl)(μ-OSi^{t}Bu$_3$)]$_4$ (1). Slow evaporation of a benzene solution of **1** yielded royal-purple rod crystals suitable for X-ray analysis. One 0.4 × 0.2 × 0.025-mm^3 crystal was selected, coated in polyisobutylene, and placed under a 173 K nitrogen stream on the goniometer head of a Siemens SMART CCD area detector system equipped with a fine-focus molybdenum X-ray tube ($\lambda = 0.71073$ Å). Preliminary diffraction data revealed a monoclinic crystal system. A hemisphere routine was used for data collection. The data were subsequently processed with the Bruker SAINT program to yield 8203 reflections of which 3478 were symmetry-independent ($R_{int} = 0.0605$). The space group was determined to be $C2/c$ with the asymmetric unit consisting of $C_{24}H_{54}O_2Si_2Cl_2Cr_2$. The data were corrected for absorption with SADABS. The structure was solved by direct methods, completed by subsequent difference Fourier syntheses, and refined by full-matrix least-squares procedures (SHELXTL). All of the non-hydrogen atoms were refined with anisotropic displacement parameters, and hydrogen atoms were included at calculated positions. The anisotropic displacement parameters for the carbon atoms indicated significant disorder in the ^{t}Bu$_3$Si groups, but a suitable disorder model could not be applied to the refinement. The presence of significant disorder that could not be modeled left large peaks (largest diff. peak = 2.277 eÅ^3) and holes (largest diff. hole = −2.571 eÅ^3) in the Fourier difference map and led to a poor refinement goodness-of-fit. The inorganic core of **1** exhibited reasonable anisotropic displacement parameters and was stable during refinement, thus establishing the overall framework of the chromous box.

8. [(^{t}Bu$_3$SiO)Cr(μ-OSi^{t}Bu$_3$)$_2$]Na·C_6H_6 (4). Slow evaporation of a benzene solution of **4** yielded faint-blue crystals suitable for X-ray analysis. One 0.4 × 0.3 × 0.15-mm^3 crystal was selected, coated in polyisobutylene, and placed under a 173 K nitrogen stream on the goniometer head of a Siemens SMART CCD area detector system equipped with a fine-focus molybdenum X-ray tube ($\lambda =$ 0.71073 Å). Preliminary diffraction data revealed a monoclinic crystal system. A hemisphere routine was used for data collection. The data were subsequently processed with the Bruker SAINT program to yield 46 138 reflections of which 10 052 were symmetry-independent ($R_{int} = 0.0469$). The space group was determined to be $P2_1/n$ with the asymmetric unit consisting of $C_{42}H_{87}Si_3O_3NaCr$. The data were corrected for absorption with SADABS. The structure was solved by direct methods, completed by subsequent difference Fourier syntheses, and refined by full-matrix least-squares procedures (SHELXTL). Two of the ^{t}Bu groups on ^{t}Bu$_3$Si(1) were disordered, and the disorder was modeled by partially occupying two ^{t}Bu groups rotationally disordered from one another. All of the non-hydrogen atoms were refined with anisotropic displacement parameters, and hydrogen atoms were included at calculated positions.

9. [(^{t}Bu$_3$SiO)$_3$Cr][Na(dibenzo-18-crown-6)] (5). In a drybox, a 4-dram vial was charged with a solution of **5** (100 mg), dibenzo-18-crown-6 (46 mg), and benzene (3 mL). Crystals suitable for X-ray analysis slowly precipitated over 12 h. A few milligrams of crystals were suspended in polyisobutylene and a 0.4 × 0.3 × 0.2-mm^3 crystal was isolated in a rayon fiber epoxied to a metal fiber and placed under a 173 K nitrogen stream on the goniometer head of a Siemens SMART CCD area detector system equipped with a fine-focus molybdenum X-ray tube ($\lambda = 0.71073$ Å). Preliminary diffraction data revealed a monoclinic crystal system. A hemisphere routine was used for data collection. The data were subsequently processed with the Bruker SAINT program to yield 29 098 reflections of which 14 829 were symmetry-independent ($R_{int} =$ 0.0371). The space group was determined to be $P2_1/n$ with the asymmetric unit consisting of $C_{133}H_{231}Si_6O_{18}Na_2Cr_2$, yielding a calculated density of 1.131 g/cm^3. The data were corrected for absorption with SADABS. The structure was solved by direct methods, completed by subsequent difference Fourier syntheses, and refined by full-matrix least-squares procedures (SHELXTL). (^{t}Bu$_3$SiO)$_3$Cr1B was heavily disordered. The ^{t}Bu group with tertiary carbon C1B and all of the ^{t}Bu groups connected to Si2B exhibited rotational disorder around the Si−C axis. The rotational disorder of each ^{t}Bu was modeled by independently refining the occupancy of two sets of methyl groups constrained to reasonable C−C bond distances. Each of the occupancies for ^{t}Bu disorder around Si2B independently refined to approximately 66:34, giving us confidence that the disorder model was reasonable. In addition, both Cr1 and Cr1B possessed a disordered Si^{t}Bu$_3$ group that contained both the ^{t}Bu rotational disorder described above combined with Si^{t}Bu$_3$ rotational disorder around the Si−O axis. The net disorder model appeared as a propeller-like structure with each pair of disordered ^{t}Bu groups sharing two methyl carbons. The occupancies of each of the two remaining methyl groups and quaternary carbons were independently refined to test the model. Reassuringly, the occupancies for the carbons disordered around Si3B all refined to approximately 50:50, whereas those around Si1 refined to approximately 70:30. All of the non-hydrogen atoms were refined with anisotropic displacement parameters except for carbons C4M, C14C, and C15C, which were unstable toward anisotropic refinement, presumably because of disorder problems. Hydrogen atoms were included at the calculated positions.

10. (^{t}Bu$_3$SiO)$_3$Cr (6). Slow evaporation at −30 °F of a saturated pentane solution of **6** yielded emerald-green crystals suitable for X-ray analysis. A few crystals were suspended in polyisobutylene, and a 0.5 × 0.3 × 0.2-mm^3 crystal was isolated in a rayon fiber epoxied to a metal fiber and placed under a 143 K nitrogen stream on the goniometer head of a Siemens SMART CCD area detector system equipped with a fine-focus molybdenum X-ray tube ($\lambda =$ 0.71073 Å). Preliminary diffraction data revealed a monoclinic crystal system. A hemisphere routine was used for data collection. The data were subsequently processed with the Bruker SAINT program to yield 50 286 reflections of which 10 639 were symmetry-independent ($R_{int} = 0.0584$). The space group was determined

to be *C*2/*c* with the asymmetric unit consisting of $C_{36}H_{81}Si_3O_3Cr$, yielding a calculated density of 1.083 g/cm^3. The data were corrected for absorption with SADABS. The structure was solved by direct methods, completed by subsequent difference Fourier syntheses, and refined by full-matrix least-squares procedures (SHELXTL). All of the non-hydrogen atoms were refined with anisotropic displacement parameters, and hydrogen atoms were included at the calculated positions.

Computational Methods. All quantum mechanics and hybrid quantum mechanics/molecular mechanics (QM/MM) calculations were carried out using the Gaussian 98[17] suite of programs. Calculations were carried out on $Cr(silox)_3$ (**6′**), $Cr(silox)_3^-$ (**5′**), and $NaCr(silox)_3$ (**4′**) using a hybrid QM/MM approach, as implemented in the ONIOM[27] methodology. The $Cr(OSi)_3$ core was modeled at the UB3PW91/6-31G level of theory.[26] The remaining *tert*-butyl groups were modeled using the universal force field (UFF).[28] For the Na^+ salt, the sodium ion was also included in the QM region.

Acknowledgment. Support from the National Science Foundation (CHE-0212147/CHE-0415506 (P.T.W.) and CHE-0309811 (T.R.C.)) and Cornell University is gratefully acknowledged. We thank Professors Roald Hoffmann and Frank J. DiSalvo for informative conversations.

Supporting Information Available: Data in CIF format. This material is available free of charge via the Internet at http://pubs.acs.org.

IC0488334